JOURNAL OF MATERIALS SCIENCE **34** (1999) 5525–5532

Reaction between Si_3N_4 and Fe-Ni alloy

T. SHIMOO, K. OKAMURA
Department of Metallurgy and Materials Science, College of Engineering, Osaka Prefecture University, Gakuen-cho, Sakai-shi, Osaka 599-8531, Japan

T. YAMASAKI
Graduate Student, Osaka Prefecture University, Gakuen-cho, Sakai-shi, Osaka 599-8531, Japan

In relation to the joining of silicon nitride ceramics to metal, the reaction between Si_3N_4 and Fe-Ni alloy was investigated under a nitrogen or an argon atmosphere at temperatures from 1123 to 1573 K. Reaction rates were determined by thermogravimetry and reaction products were examined by X-ray diffraction. Fe-Ni-Si solid solution, Ni_3Si, Ni_5Si_2, $NiSi_2$, Fe_3Si, Fe_5Si_3 and FeSi were produced. The initial rate obeyed a linear rate law. The rate at the late stage of reaction was described by a parabolic rate law or Fick's second law. The reaction mechanism and the rate-determining step were proposed.

1. Introduction

Silicon nitride (Si_3N_4) has attracted much attention as a high-temperature structural ceramic because of its excellent thermal and mechanical properties. However, it is brittle and machines poorly. In addition, complex-shaped and large-sized components are difficult to fabricate. These disadvantages can be lessened by joining the ceramic to metal [1–8]. A reaction layer is formed at the silicon nitride/metal interface during joining treatment, and grows further in high-temperature service of the joints. Excessive growth of the reaction layer results in chemical degradation of the joint. Thus, examination of the reaction products and reaction mechanism between silicon nitride and metal can provide useful insights into ceramic/metal bonding.

Since commercially available ceramics and metals contain sintering additives and alloying elements, the reaction behavior between both materials is greatly complicated. In addition, the reaction between block samples is very sluggish. From such a viewpoint, the authors have investigated the relative chemical reactivity of Si_3N_4 with a number of pure metals, using powder samples [9–19]. From this result, it is possible to project the condition of the ceramic/metal bond after long-time service at high temperatures. Fe-Ni alloy is important as a basic type of heat-resistant steel. Therefore, the reactivity of Si_3N_4 with Fe-Ni alloy at high temperature is of great interest. In this work, the reaction kinetics of Si_3N_4 powder with Fe-Ni alloy powder has been studied, and the reaction products and reaction mechanism were revealed.

2. Experimental

The starting materials were silicon nitride powder (Ube Industries Ltd., α fraction $\geqq$95, purity 98.5%, average particle size 0.2 μm) and Fe-46.9mass%Ni alloy powder (Kobe Steel Ltd., purity 99.7%, average particle size 9 μm). This alloy powder is called Fe46Ni. A mixture of 2g Si_3N_4 and 2g Fe46Ni alloy was thoroughly mixed in a silicon nitride mortar and compacted into a tablet of 20 mm diameter.

The thermobalance unit used for thermogravimetry (TG) consisted of a digital-type automatic recording balance (measurable limit 100 g, sensitivity 0.1 mg) and an SiC resistance furnace. When the desired temperature was reached, either nitrogen or argon was flowed from the bottom of the furnace at 2.5×10^{-5} $m^3 \cdot s^{-1}$. A tablet specimen was placed in a magnesia crucible (inner diameter 26 mm, depth 35 mm). The magnesia crucible was suspended in the hot zone of the furnace (alumina reaction tube of 44 mm inner diameter) with a platinum wire connected to a balance. The mass change was recorded automatically during each experiment. Upon completion of the measurement, the specimen was quenched by raising the crucible into the low-temperature zone of the furnace. The reaction products were analyzed by X-ray diffraction.

3. Result

3.1. TG curves

Fig. 1 shows the mass changes for Si_3N_4-Fe46Ni mixtures which were heated continuously from room temperature to 1573 K at a heating rate of 1 K/min. $100 \cdot \Delta W / W_0$ is the ratio of the mass loss determined by TG to the initial mass of sample. Under both nitrogen and argon atmospheres, the mass loss begins at about 1260 K. Interestingly, this temperature is between 1320 K for Si_3N_4-Fe and 950 K for Si_3N_4-Ni [10, 11]. The subsequent mass loss is more vigorous under an argon than under a nitrogen atmosphere. As stated later,

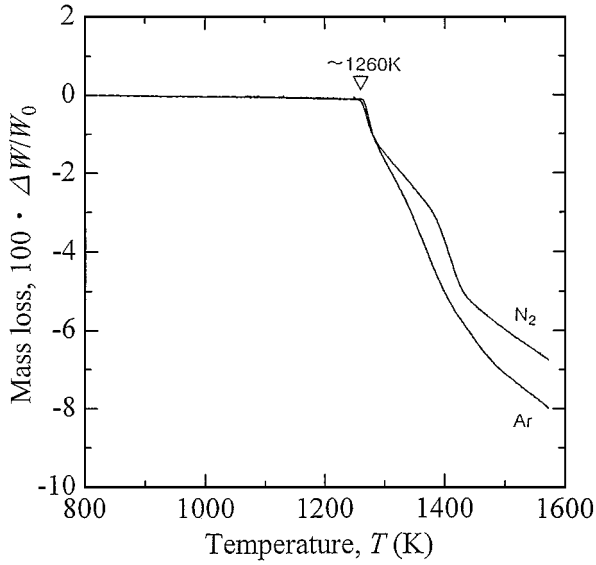

Figure 1 Mass loss with reaction of Si_3N_4-Fe46Ni mixture heated continuously at 1 K/min.

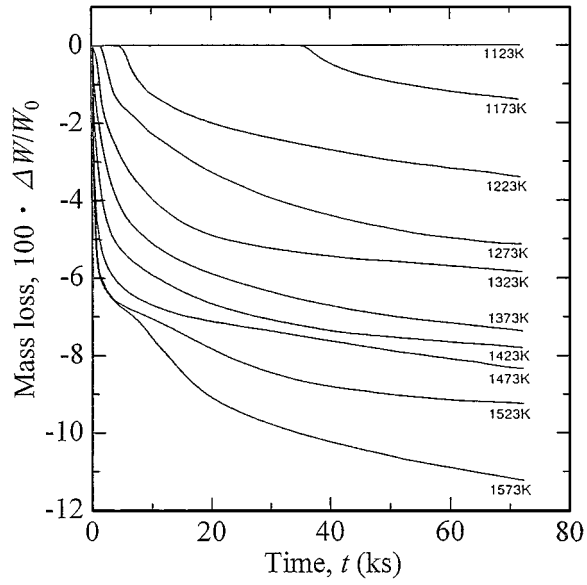

Figure 3 Mass loss with reaction of Si_3N_4-Fe46Ni mixture heated isothermally under an argon atmosphere at temperatures from 1123 to 1573 K.

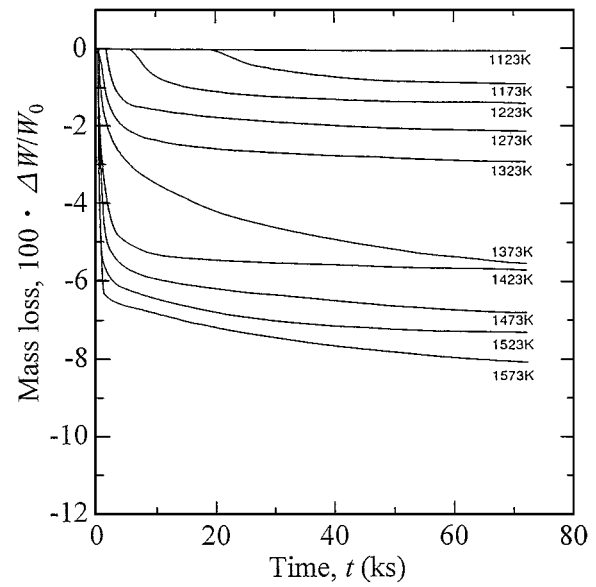

Figure 2 Mass loss with reaction of Si_3N_4-Fe46Ni mixture heated isothermally under a nitrogen atmosphere at temperatures from 1123 to 1573 K.

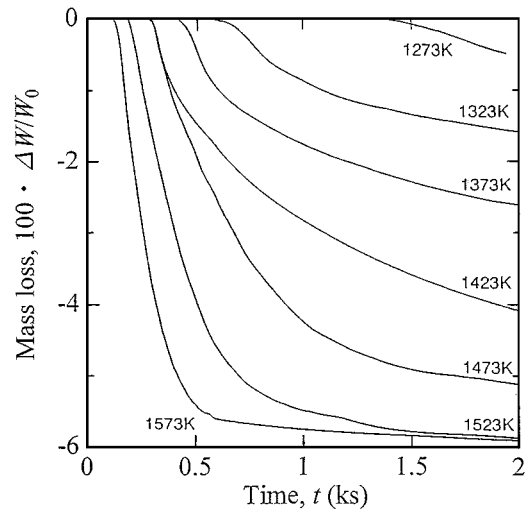

Figure 4 Incubation period for reaction of Si_3N_4-Fe46Ni mixture heated isothermally under a nitrogen atmosphere.

the mass loss is due to the formation of a solid solution and silicides, accompanied by the generation of nitrogen gas.

Figs 2 and 3 show TG curves for Si_3N_4-Fe46Ni mixtures heated isothermally at temperatures from 1123 to 1573 K under a nitrogen and an argon atmosphere, respectively. A substantial incubation period is observed at low temperatures. A brief incubation period is found even at higher temperatures, as shown in Fig. 4. At 1123 K, the reaction does not occur at all. This may be because the incubation period is longer than the experiment time. Under both atmospheres, the reaction occurs rapidly after the incubation period and then the reaction rate decreases gradually. It may be noted that each TG curves under a nitrogen atmosphere has a tendency to converge on a particular value.

3.2. X-ray diffraction

Figs 5 and 6 show the relative X-ray intensities of the reaction products after heating Si_3N_4-Fe46Ni mixtures for 72 ks. The relative X-ray intensity is the ratio of the strongest intensity for each product to that for Si_3N_4 (2 0 0). Under a nitrogen atmosphere and at 1373 K, Ni_5Si_2 and Fe_3Si are simultaneously produced with disappearance of Fe46Ni alloy (γ phase). Then, Ni_2Si is produced at 1523 K. Under an argon atmosphere, silicides were produced in the following order: Ni_5Si_2 and Fe_3Si at 1223 K, Ni_2Si at 1323 K, Fe_5Si_3 at 1473 K and FeSi at 1523 K. Under both atmospheres, the diffraction peaks of Fe46Ni alloy (γ phase) were shifted to the high-angle side with increasing the temperature. This is because silicon forms a substitutional solid solution with γ phase. Consequently, the lattice constant of γ phase decreases, as shown in Fig. 7. Ultimately, silicides precipitate from super saturated solid solution. The Si/metal ratio of the silicides increased with

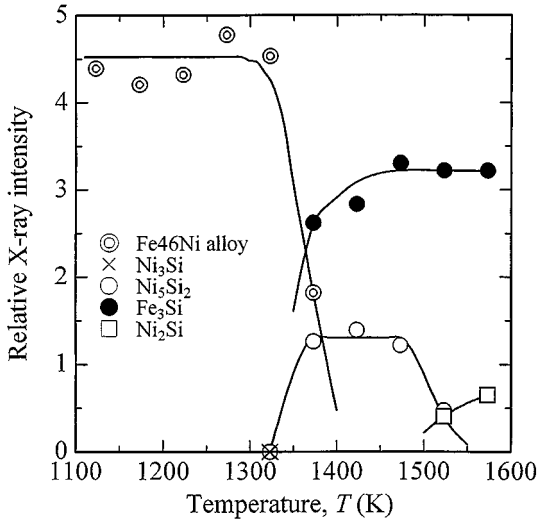

Figure 5 Relative X-ray intensities of reaction products in Si_3N_4-Fe46Ni mixture heated for 72 ks under a nitrogen atmosphere.

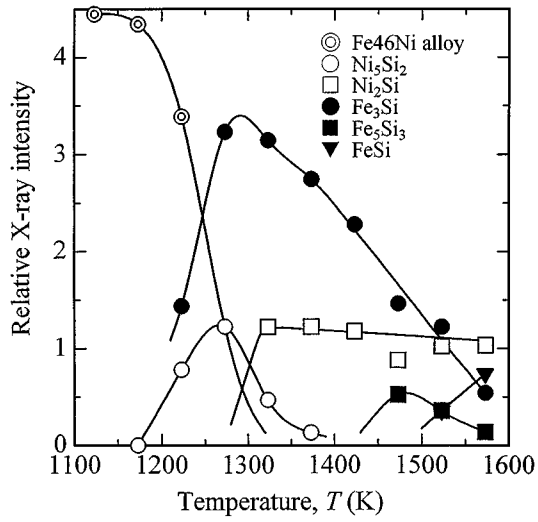

Figure 6 Relative X-ray intensities of reaction products in Si_3N_4-Fe46Ni mixture heated for 72 ks under an argon atmosphere.

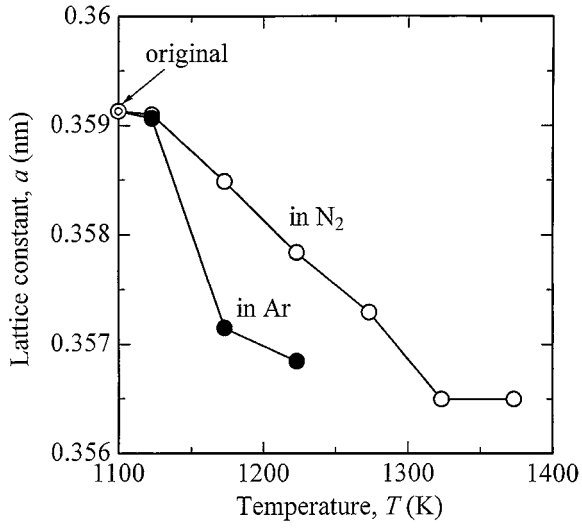

Figure 7 Lattice constant of γ phase (Fe-Ni-Si solid solution) in Si_3N_4-Fe46Ni mixture heated for 72 ks.

TABLE I Reaction products in Si_3N_4-Fe46Ni mixture heated under a nitrogen atmosphere (detected by X-ray diffraction)

Temperature T(K)	Time t(ks)	Si_3N_4	Fe46Ni	Ni_3Si	Ni_5Si_2	Fe_3Si
1273	0.9	○	○	×	×	×
	7.2	○	○	×	×	×
	18	○	○	×	×	×
	72	○	○	×	×	×
1323	0.9	○	○	×	×	×
	3.6	○	○	×	×	×
	7.2	○	○	△	△	×
	18	○	○	△	△	×
	72	○	○	△	△	×
1373	0.9	○	○	△	△	×
	7.2	○	○	△	○	○
	18	○	○	×	○	○
	72	○	○	×	○	○

○: strong; △: very weak; ×: undetected.

temperature and heating time. Ni_3Si which has lower Si/metal ratio than Ni_5Si_2 was not detected by X-ray diffraction. This is thought to be because the diffraction intensity of Ni_3Si was very weak. Therefore, metal particles were separated from sample by allowing Si_3N_4 powder to suspend in acetone and were submitted to X-ray diffraction. The X-ray diffraction pattern of this metal particles is shown in Fig. 8. Very small peaks of Ni_3Si were detected. Their X-ray intensity was about 10^4 times less than that of γ phase (1 1 1). Table I shows the phase detected by this method. A slight amount of Ni_3Si is found to form only under limited conditions.

4. Discussion

4.1. Reaction products

On isothermal heating of Si_3N_4-Fe46Ni compacts, reaction proceeded above 1173 K under both nitrogen and argon atmospheres, although an incubation period was observed (Figs 2–4). Both iron and nickel do not produce nitrides at the experimental temperatures [20]. In addition, nitrogen hardly forms a solid solution with iron and nickel [20]. Therefore, the reaction products between Si_3N_4 and Fe46Ni are the Fe-Ni-Si solid solution and silicides of iron and nickel. As can be seen from Figs 2, 3 and 7, a mass loss was observed and the lattice constant of Fe46Ni alloy (γ phase) decreased at temperatures of 1173 K and higher, under both nitrogen and argon atmospheres. This indicates that γ phase forms a solid solution with silicon. The reaction and standard free energy change, ΔG^0, for formation of solid solution are given by

$$Si_3N_4(s) = 3\underline{Si} + 2N_2(g) \quad (1)$$

$$\Delta G^0/\mathrm{J \cdot mol^{-1}} = 723800 - 315T/\mathrm{K}\ [21]$$

where $\underline{Si}$ stands for silicon which forms the solid solution. The Raoultian activity relative to pure silicon is employed as the activity of $\underline{Si}$, a_{Si}. Under a nitrogen atmosphere, Si_3N_4 decomposes to pure silicon ($a_{Si} = 1$)

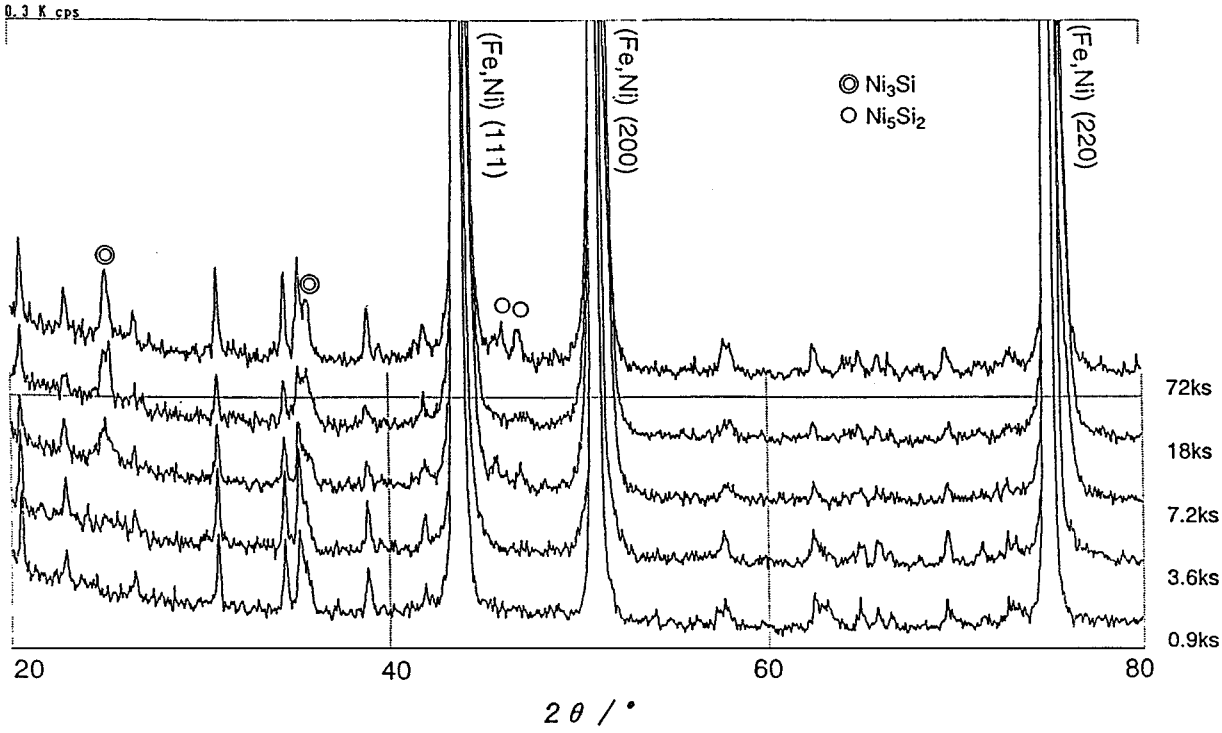

Figure 8 X-ray diffraction patterns of Fe46Ni alloy powder reacted with Si_3N_4 at 1323 K under a nitrogen atmosphere.

above 2298 K. Therefore, the reaction between Si_3N_4 and Fe46Ni alloy produced the solid solution having low activity at the experimental temperatures. For example, the formation of the solid solution with a_{Si} of 5.5×10^{-6} and smaller is possible at 1173 K. Under an argon atmosphere, a solid solution with still higher activity will be produced because of the low nitrogen pressure.

At higher temperatures, Figs 5 and 6 indicate the formation of nickel silicides (Ni_3Si, Ni_5Si_2 and Ni_2Si) and iron silicides (Fe_3Si, Fe_5Si_3 and FeSi). The Si/metal ratio of the silicides increases with increasing temperature and heating time. The silicides with a low Si/metal ratio react with Si_3N_4 to produce those with a high Si/metal ratio. Reactions for the formation of silicides are represented by

$$9\underline{Fe} + Si_3N_4(s) = 3Fe_3Si(s) + 2N_2(g) \quad (2)$$

$$\Delta G^0/J \cdot mol^{-1} = 298800 - 215T/K \text{ [21]}$$

$$15Fe_3Si(s) + 4Si_3N_4(s) = Fe_5Si_3(s) + 8N_2(g) \quad (3)$$

$$3Fe_5Si_3(s) + 2Si_3N_4(s) = 15FeSi(s) + 4N_2(g) \quad (4)$$

$$9\underline{Ni} + Si_3N_4(s) = 3Ni_3Si(s) + 2N_2(g) \quad (5)$$

$$\Delta G^0/J \cdot mol^{-1} = 308900 - 329T/K \text{ [22]}$$

$$15Ni_3Si(s) + Si_3N_4(s) = 9Ni_5Si_2(s) + 2N_2(g) \quad (6)$$

$$6Ni_5Si_2(s) + Si_3N_4(s) = 15Ni_2Si(s) + 2N_2(g) \quad (7)$$

where Fe and Ni stand for iron and nickel which form the solid solution. The activities of iron and nickel in the alloy, a_{Fe} and a_{Ni}, are the Raoultian activities relative to pure iron and nickel. Since Fe-Ni alloy may be approximately regarded as an ideal solution [23], the activity is equal to the concentration (mole fraction). Therefore, a_{Fe} and a_{Ni} of Fe46Ni alloy are equal to 0.54 and 0.46, respectively. Under a nitrogen atmosphere, Ni_3Si and Fe_3Si are thermodynamically produced at 1140 and 1768 K, respectively. Therefore, Ni_3Si is the earliest product. X-ray diffraction also shows that Ni_3Si is at first produced at 1323 K. The observed temperature is appreciably higher than the thermodynamically estimated temperature of 1140 K. This seems to be because the formation of Ni_3Si is accompanied by a diffusion process (reaction diffusion). Its diffraction intensity remains very weak and finally disappears at 1373 K. According to the phase rule, this result is explicable as stated below.

The Fe-Ni-Si phase diagram at 1273 K is shown in Fig. 9 [24]. The initial composition of Fe46Ni alloy is represented at point A. The reaction between Si_3N_4 and Fe46Ni alloy leads to the shift of alloy composition in the direction of the arrow. That is, the composition changes γ single-phase to the γ + b.c.c. + Ni_5Si_2 three-phase field. The b.c.c. phase is either a solid solution or Fe_3Si [24]. Even though Ni_3Si is produced, further growth of Ni_3Si is unlikely as can be seen from Fig. 9. Therefore, the very weak diffraction intensity of Ni_3Si was found only at 1323 and 1373 K under a nitrogen atmosphere (Table I). Thus, for the reaction between Si_3N_4 and Fe46Ni alloy, Fe_3Si and Ni_5Si_2 are simultaneously produced and grow as stable phases, corresponding to the phase diagram. On the other hand, for the reaction between Si_3N_4 and pure nickel, which is free from the restriction by the above phase rule, Ni_3Si appears at 1073 K and continues to grow until Ni_5Si_2 is produced at 1223 K [9, 10].

From Equation 2, the temperature of Fe_3Si formation is thermodynamically calculated to be 1768 K for Fe64Ni alloy with a_{Fe} of 0.54. The observed value of 1373 K is much lower than the calculated value. Iron excluded by the preferential formation of Ni_3Si and

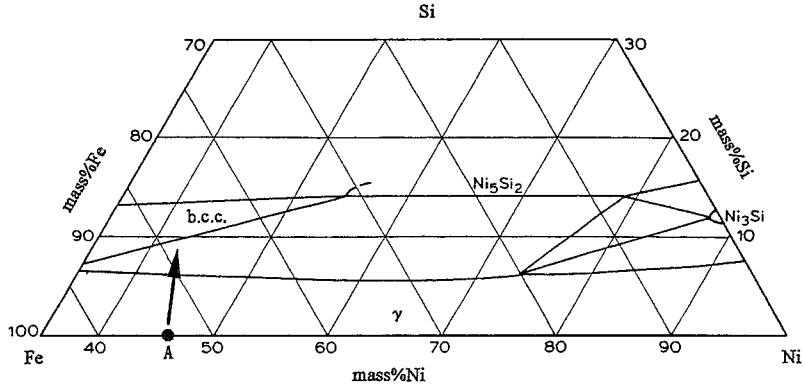

Figure 9 Fe-Ni-Si ternary system at 1273 K, after Ref. 24. Point A corresponds to Fe46Ni alloy.

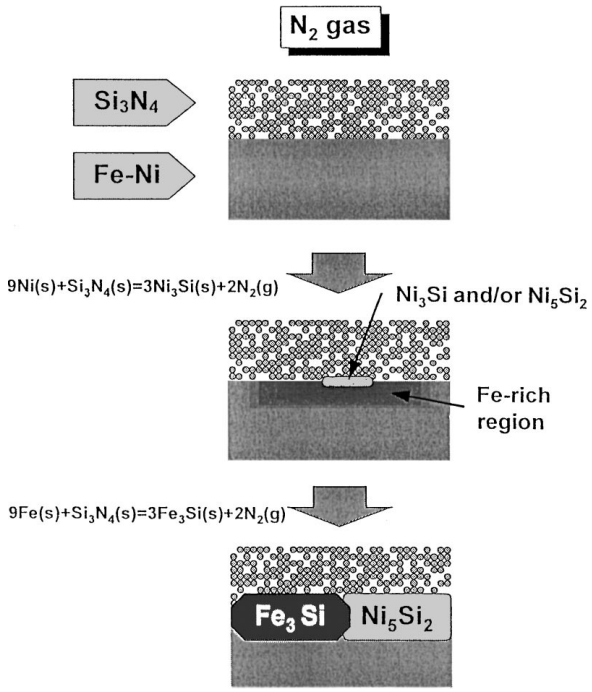

Figure 10 Schematic illustration of reaction process between Si_3N_4 and Fe46Ni under a nitrogen atmosphere.

Ni_5Si_2 is enriched in the alloy, as shown in Fig. 10. The a_{Fe} in the enriched region is nearly equal to unity. Consequently, Fe_3Si is thermodynamically estimated to be produced above 1390 K. The temperature for Fe_3Si formation is somewhat higher than the experimentally determined temperature of 1373 K (Fig. 5), arising from the error in ΔG^0. Interestingly, the reaction between Si_3N_4 and pure iron ($a_{Fe} = 1$) also produced Fe_3Si at 1373 K under a nitrogen atmosphere [11].

Under an argon atmosphere, the simultaneous formation of Fe_3Si and Ni_5Si_2 occurred at the lower temperature of 1223 K, because of a low nitrogen pressure. At elevated temperature, the silicides with higher Si/metal ratios were produced ; Ni_2Si, Fe_5Si_3 and FeSi.

4.2. Reaction mechanism and rate-determining step

At the early stage of the reaction between Si_3N_4 and metal, the rate data obeyed the following linear rate equation [10, 14, 16, 17]

$$100 \cdot \Delta W / W_0 = k_1 \cdot t \qquad (8)$$

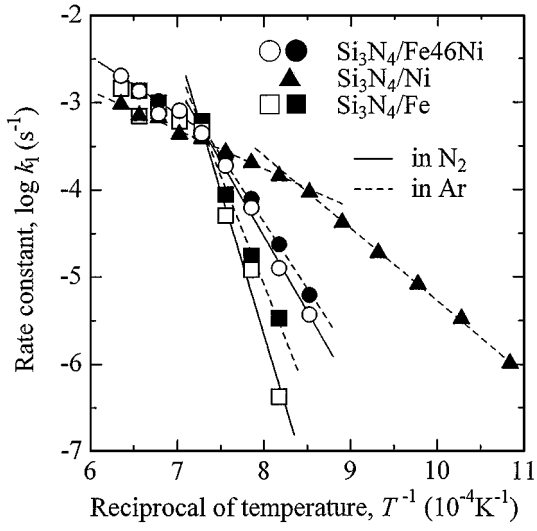

Figure 11 Arrhenius plots for rate constant k_1 of linear rate law.

The linear rate constant, k_1 is obtained from the initial linear regions of TG curves given in Figs 2 and 3. Fig. 11 indicates the Arrhenius plots of k_1. The values of k_1 in Si_3N_4-Ni and Si_3N_4-Fe are shown for comparison with k_1 in Si_3N_4-Fe46Ni alloy. The slope of the Arrhenius line is different above and below 1373 K for Si_3N_4-Fe46Ni. The activation energies at lower temperatures were estimated to be 346 $kJ \cdot mol^{-1}$ under a nitrogen atmosphere and 315 $kJ \cdot mol^{-1}$ under an argon atmosphere. These values are reasonable for the activation energy of a chemical reaction. The value of k_1 is smaller under a nitrogen than under an argon atmosphere, reflecting that the interfacial reaction produces the evolution of nitrogen gas. At higher temperatures, the low activation energy of 106 $kJ \cdot mol^{-1}$ was obtained regardless of atmosphere. The low activation energy suggests that the diffusion of nitrogen gas through interparticle pores in the Si_3N_4-Fe46Ni mixture is the rate-determining step. At low temperature, the initial rate is considered to be controlled by reaction at the interface between Si_3N_4 and Fe46Ni alloy. At higher temperatures, rapid progress of the interfacial reaction generates nitrogen gas. Consequently, the rate-determining step shifts from interfacial reaction to gaseous diffusion in the pores of the compact. A similar reaction mechanism will be presented also for Si_3N_4-Fe and Si_3N_4-Ni.

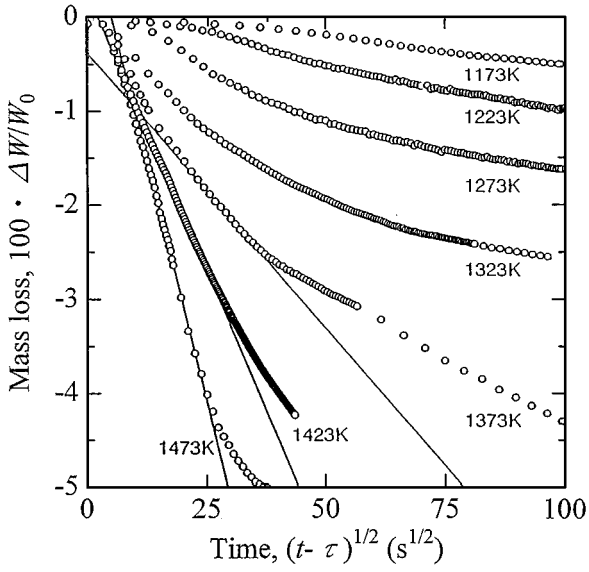

Figure 12 Application of parabolic rate law to kinetic data shown in Fig. 2.

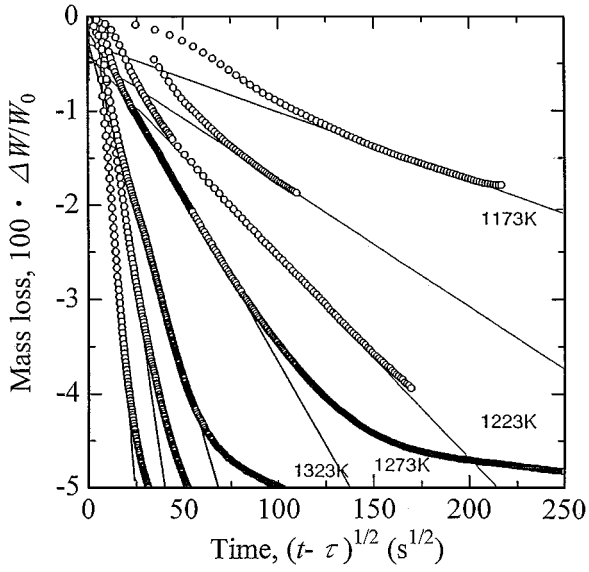

Figure 13 Application of parabolic rate law to kinetic data shown in Fig. 3.

The TG curves initially obey a linear rate law and then gradually deviate from it. The kinetics at the late stage can be expressed by a parabolic rate law [10, 14, 16, 17]

$$100 \cdot \Delta W / W_0 = k_p^{1/2} \cdot (t - \tau)^{1/2} \qquad (9)$$

where is the parabolic rate constant and τ is the incubation period. As shown in Figs 12 and 13, the plots satisfy the parabolic rate equation above 1373 K under a nitrogen atmosphere and over the entire temperature range under an argon atmosphere when $100 \cdot \Delta W/W_0 \geqq -1$. Fig. 14 shows Arrhenius plots of the parabolic rate constant, k_p. The value of k_p is independent of the atmosphere. The calculated activation energy of 337 $kJ \cdot mol^{-1}$ is nearly the same as that obtained for the reaction of Si_3N_4 with other metals [10–12, 16, 17]. When the metal particles are completely coated with the product layer, subsequent reaction between Si_3N_4 and metal involves solid-state diffusion.

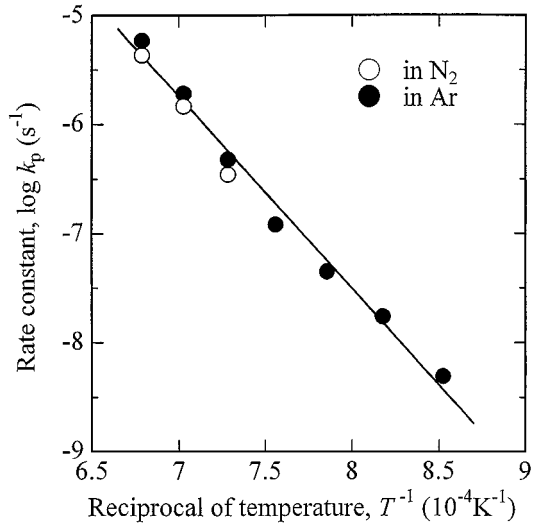

Figure 14 Arrhenius plots for rate constant k_p of parabolic rate law.

The above results substantiate solid-state diffusion control through the product layer.

Under a nitrogen atmosphere and below 1323 K, the parabolic rate law was inapplicable to the kinetic data. In addition, the reaction product was only the Fe-Ni-Si solid solution. With the assumption that unsteady state diffusion occurs through alloy particles, Fick's second law of diffusion is applied to the kinetic data [25]. The concentration of silicon is initially zero throughout the Fe46Ni alloy particle and its surface is maintained at a constant concentration during reaction with Si_3N_4. Under the above conditions, solving Fick's second law yields the following result [25]:

$$M_t/M_\infty = 1 - 6/\pi^2 \sum_{n=1}^{\infty} 1/n^2 \times \int_0^\infty f(a) \cdot \exp(-Dn^2\pi^2 t/a^2) \qquad (10)$$

where M_t and M_∞ are the quantity of diffusing substance leaving the sphere in time t and after infinite time, respectively. In addition, D is the diffusion coefficient, a is the particle radius and $f(a)$ is a density function for the distribution of the particle sizes. $f(a)$ can be estimated because the particle sizes of Fe46Ni alloy obey the logarithmic normal distribution as shown in Fig. 15. The values of D and M_∞ were determined by trial and error so that the calculated results fit with the TG curves. The value of M_∞ corresponds to the solid solubility in Fe46Ni alloy at each temperature. Fig. 16 shows the simulated curves (dashed line), together with the TG curves. Good agreement between the curves is observed. However, such simulations cannot be carried out using Equation 10 when silicides are produced. Arrhenius plots of D are shown in Fig. 17. The plots display good linearity. For the temperature range from 1173 to 1323 K, the value of D varies from 4.3×10^{-17} to 5.2×10^{-16} $m^2 \cdot s$. While the value of D in Fe-Ni-Si is the same as D in Fe-Ni [23] and Ni-Si [26], it is 3 orders of magnitude lower than D in Fe-Si [27]. The activation energy calculated from

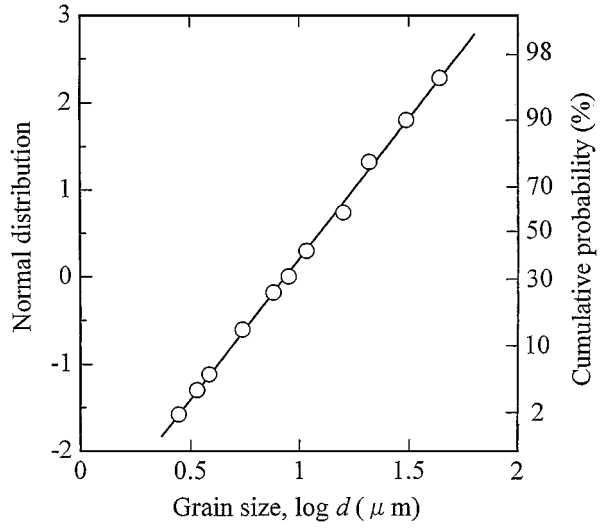

Figure 15 Normal distribution for particle size of Fe46Ni alloy powder.

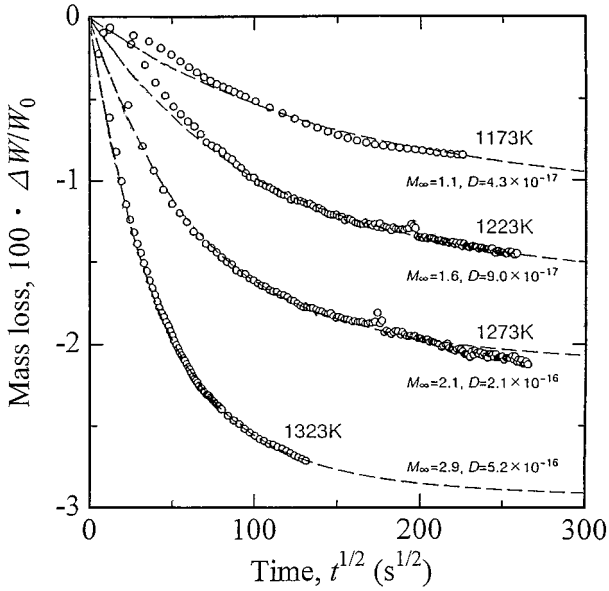

Figure 16 Application of Equation 10 to kinetic data shown in Fig. 2.

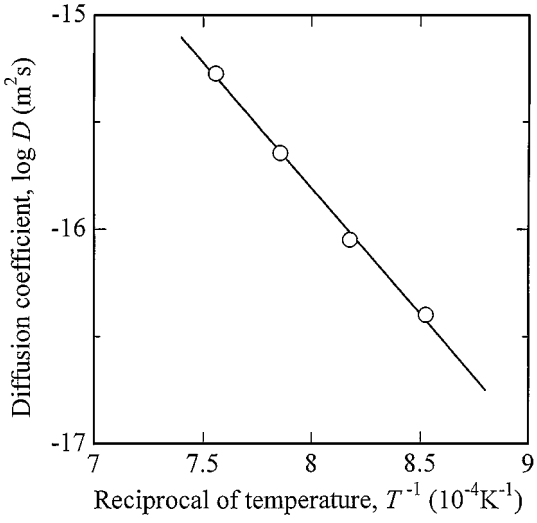

Figure 17 Arrhenius plots for diffusion coefficient D.

the slope of the Arrhenius line is 236 kJ · mol^{-1}. This value is roughly comparable with 258 kJ · mol^{-1} for Ni-Si [26] and 209 kJ · mol^{-1} for Fe-Si [27], though it is appreciably lower than 317 kJ · mol^{-1}for Fe-Ni [23].

5. Conclusion

The reaction between Si_3N_4 and Fe-46.9mass%Ni alloy was investigated by thermogravimetry and X-ray diffraction methods in order to reveal the reaction products and reaction mechanisms. Compacts of Si_3N_4/alloy powder mixture were heated for 72 ks at temperatures from 1123 to 1573 K under a nitrogen or an argon atmosphere.

1. The formation of an Fe-Ni-Si solid solution begin at 1173 K under both atmospheres.
2. Under a nitrogen atmosphere, a slight amount of Ni_3Si was produced at 1323 and 1373 K. Above 1373 K, Ni_5Si_2 and Fe_3Si were simultaneously produced corresponding to the Fe-Ni-Si phase diagram.
3. Under an argon atmosphere, both Ni_5Si_2 and Fe_3Si were produced at 1223 K. With increasing temp erature, the Si/metal ratio of the silicides increased in the sequence $Ni_5Si_2 \rightarrow Ni_2Si$ and $Fe_3Si \rightarrow Fe_5Si_3 \rightarrow$ FeSi.
4. A long incubation period was observed at 1123 K. The incubation period was shortened with increasing temperature.
5. The initial reaction rate obeyed a linear rate law. The reaction rate below 1323 K is determined by reaction at the interface between Si_3N_4 and Fe-Ni alloy, whereas the rate above 1373 K is controlled by gaseous diffusion of nitrogen through interparticle pores in the compact.
6. The rate was described by a parabolic rate law at late stages of reaction, when alloy particles were completely coated by the reaction layer. The rate data under a nitrogen atmosphere and below 1323 K were analyzed by Fick's second law. The reaction rate is considered to be controlled by solid-state diffusion through the reaction layer.

Acknowledgement

This study was supported partly by a grant from Tanikawa Fund of Thermal Technology, which is gratefully acknowledged.

References

1. R. E. LOEHMAN and A. P. TOMSIA, *Amer. Ceram. Soc. Bull.* **67** (1988) 375.
2. S. KANG, E. M. DUNN, J. H. SELVERIAN and H. J. KIM, *Amer. Ceram. Soc. Bull.* **68** (1989) 1608.
3. G. ELSSNER and G. PETZOW, *ISIJ International* **30** (1990) 1011.
4. T. OKAMOTO, *ibid.* **30** (1990) 1033.
5. K. SUGANUMA, *ibid.* **30** (1990) 1046.
6. O. M. AKSELSEN, *J. Mater. Sci.* **27** (1992) 569.
7. *Idem., ibid.* **27** (1992) 1989.
8. J. M. HOWE, *International Mater. Rev.* **38** (1993) 233.

9. T. SHIMOO, T. KIYA and K. OKAMURA, *Nippon Kinzokugakkai-shi* **55** (1991) 796.
10. T. SHIMOO, Y. KOBAYASHI and K. OKAMURA, *J. Ceram. Soc. Jpn* **100** (1992) 808.
11. T. SHIMOO, Y. MORIUCHI and K. OKAMURA, *Nippon Kinzokugakkai-shi* **56** (1992) 1030.
12. T. SHIMOO, Y. KOBAYASHI and K. OKAMURA, *ibid*. **57** (1993) 561.
13. *Idem., J. Ceram. Soc. Jpn* **101** (1993) 675.
14. *Idem., ibid*. **101** (1993) 1012.
15. T. SHIMOO and K. OKAMURA, *J. Mater. Sci*. **29** (1994) 2231.
16. T. SHIMOO, S. ADACHI and K. OKAMURA, *Nippon Kinzokugakkai-shi* **58** (1994) 796.
17. T. SHIMOO, A. SANDJAJA, S. ADACHI and K. OKAMURA, *J. Ceram. Soc. Jpn* **103** (1995) 108.
18. T. SHIMOO, S. ADACHI and K. OKAMURA, *ibid*. **103** (1995) 1027.
19. T. SHIMOO, A. SANDJAJA and K. OKAMURA, *J. Jpn Soc. Powder and Powder Met*. **43** (1996) 346.
20. M. HANSEN, "Constitution of Binary Alloys" (McGraw-Hill Book, New York, 1958) pp. 670–674, pp. 984–985.
21. T. HIRAI and T. MATSUDA, *J. High Temp. Soc. Jpn* **3** (1977) 146.
22. E. T. TURKDOGAN, "Physical Chemistry of High Temperature Technology" (Academic Press, New York, 1980) pp. 5–24.
23. J. I. GOLDSTEIN, R. E. HANNEMAN and R. E. OGILVIE, *Trans. Met. Soc. AIME* **233** (1965) 812.
24. G. V. RAYNER and V. G. RIVLIN, *International Met. Rev*. **30** (1985) 181.
25. J. CRANK, "The Mathematics of Diffusion" (Clarendon Press, Oxford, 1975) pp. 90–91.
26. J. POMEY, *Mem. Sci. Rev. Metall*. **60** (1963) 215.
27. H. MITANI, M. ONISHI and M. KAWGUCHI, *Nippon Kinzokugakkai-shi* **31** (1967) 1341.

Received 20 August 1998
and accepted 27 April 1999